

https://dspace.org/

Investigation of extended and localised states in a high-temperature superconducting ceramic.

De Villiers, Patrick

2015-03-05
http://hdl.handle.net/10539/17156

Downloaded from a DSpace repository. https://dspace.org/

Figure 1.1.7 A Sharvin point contact arrangement illustrates Andreev reflection. 20

Figure 1.2.1 (a) A schematic representation of the YBCO structure emphasizing the two immediately adjacent Cu–O planes.
(b) Orthorhombic YBCO emphasizing the atomic positions. 25

Figure 1.2.2 Variation of the superconducting order parameter, Ψ. Excited and Localised states. 27

Figure 1.2.3 A superconducting circuit representing the relative motion of the extended states (ES) and the localised states (LS) resulting from an applied Lorentz force. 29

Figure 1.2.4 Schematic of "pancake type" vortices that form in layered High–T_c materials due to the weak–interlayer coupling when a magnetic field penetrates the superconductor. 32

Figure 1.2.5 A comparison of the magnetic field dependent resistivity, $\rho(H)$, for a) High–T_c superconductors and b) conventional systems. 34

Figure 1.2.6 An approximation of the characteristic E(J) behaviour for two different temperatures, T_1 and T_2. 38

Figure 2.1 A schematic of the sample mounting, showing the position of the YBCO sample with regard to the Carbon Glass Thermometer, axial Hall probe and heater. 44

Figure 2.2 Schematic of the Janis cryostat used for the measurements. 47

Figure 2.3 (a) A superconducting bar sample with current applied in the x–direction, between contact pair (1,2) and tranverse magnetic field in the z–direction.
(b) A disc–shaped Corbino geometry, with the current injected at the centre of the disc and removed from the rim. 50

Figure 2.4 A schematic representation of the equipotentiality for an ideal disc geometry and non–ideal case. 52

Figure 3.1 Corbino sample geometry displaying a typical contact pair, (R_{out}, r). 56

Figure 3.2 A typical voltage curve, W(T), superimposed on its respective $\Gamma_{\varphi}(T)$ curve to indicate the region in which the theory is fitted. 60

Figure 3.3 (a) $dW(T,B=0)/dT$ for 30 mA, $T_c(0) = 88$ K
(b) The resistive broadening of the four fields used, I = 100 mA. 62

Table 3.1 Dependence of d(R) and D(R) for the four contact arrangements; A,B,C and D. 63

Figure 3.4 Functional dependence $d(R) \equiv \mathrm{Log}[R_{out}/r]$ is illustrated by plotting the temperature derivative of the normal–state, $dw_N(T)/dT$, versus d(R) for each contact pair. 65

Figure 3.5 $W(T)/w_N(T)$ versus $(R_{out}^2 - r^2)$ for 10 mA, 0.59T at five discrete temperatures. 66

Figure 3.6 (a) Temperature dependence of α_q.
(b) Current independence of $\alpha_q(T)$. 67

Figure 3.7 (a) Least squares fit of $\alpha_q(T) = \exp[-d_S/\xi(T)]$ to the 100 mA data.
(b) A plot of $(\mathrm{Log}[\alpha_q(T)])^2$ versus T^2. 69

Figure 3.8 $\Gamma_\varphi(T,B)$ for H = 1.78 T and H = 8.29 T with excitation current of 100 mA. Solid lines are the PMTAFF fits. 71

Figure 3.9 Current dependence of $\Gamma_{\varphi}(T,B)$. 72

Figure 3.10 A plot of $\Gamma_0(J,B=8.29\ T)$ versus I 73

Table 3.2 Results tabulated for the activation energy, U(I,B) and the current dependent, $\Gamma_c(I,B)$. 76

Figure 3.11 (a) A plot of U(I,B) versus Log[I], to remove the current dependence from the activation energy.
(b) A plot of Log[U(B)] as a function of B. 78

Figure B.1 Linear fit of the form A + BT to the normal–state, $w_N(T)$. 88

Figure B.2 Quadratic fit of the form $A + BT + CT^2$, to the normal–state, $w_N(T)$. 89

CHAPTER 1

INTRODUCTION

1.1 Basic Principles of Conventional Superconductivity

Since the discovery of Superconductivity in 1911 by Onnes[1], many theoretical interpretations and classifications have evolved with the development of Type II, and much later, high T_c superconductors. Though the general definition of a superconductor relates to a material exhibiting perfect conduction and diamagnetism, there exist other very interesting aspects of superconductivity that cannot all be mentioned in this introductory overview. The most important nomenclature and theoretical background relevant to this specific study shall be dealt with.

1.1.1 Theory of Ginzburg–Landau

In 1950, Ginzburg and Landau[2] proposed a phenomenological theory of superconductivity based on the previous theory of second–order phase transitions formulated by Landau. Landau had suggested that these phase transitions could be described in terms of an order parameter. The Ginzburg–Landau, or GL Theory, introduces a complex psuedo–wave function Ψ as the order parameter, which is hypothesized to be related to the local density of superconducting electrons as

$$|\Psi|^2 = n_s$$

1.1.1.

In the presence of a magnetic field (H), the free energy density of the superconducting state, F_{sH}, near a second–order phase transition, may be expanded as follows:

$$F_{sH} = F_{n0} + \alpha|\Psi|^2 + \tfrac{1}{2}\beta|\Psi|^4 + (2m^*)^{-1}|(-i\hbar\nabla - 2eA)\,\Psi\,|^2 + h^2/8\pi \qquad 1.1.2.$$

where Ψ (r) is the complex order parameter; F_{n0} is the free energy density of the normal state in zero field; $h^2/8\pi$ is the magnetic energy density equivalent to $B^2/2\mu_0 - \mu_0 H_0^2/2$ in SI units; α, β are phenomenological constants, and m^* is an effective mass of an electron. In the presence of fields, currents and gradients, $\Psi(r) = |\Psi(r)|\exp[i\varphi(r)]$ adjusts accordingly so as to minimize the total free energy. Thus setting the variation of the free energy with respect to the order parameter equal to zero, and with the restriction that we use the gauge div A = 0, equation 1.1.2 is differentiated to obtain,

$$\alpha\,\Psi + \beta|\,\Psi\,|^2\,\Psi + \frac{1}{2m^*}(-i\hbar\nabla - 2eA)^2\,\Psi = 0 \qquad 1.1.3.$$

Along with this equation, GL obtain the usual quantum expression for the current, J = $(1/\mu_0)$ curl B (Maxwell's equation), as

$$J = -\frac{ie\hbar}{m^*}(\Psi^*\,\Psi - \Psi\,\Psi^*) - \frac{4e^2}{m^*}\Psi^*\Psi A \qquad 1.1.4.$$

A is the vector potential of any magnetic field B present, for example in the penetration region or the mixed state, defined so that

$$B = \text{curl } A \qquad 1.1.5.$$

If the dimensions of the sample are larger than the effective penetration, there exists regions where $B = 0$ inside the specimen. Hence, the spatial variation of Ψ would be zero (Ψ is a constant), and this constant value from equation 1.1.3 is

$$|\Psi|^2 = |\alpha|/\beta \qquad 1.1.6.$$

Since $\nabla \Psi = 0$, the super current, (equation 1.1.4), is given by the London equation

$$J_s = -\frac{4e^2}{m^*}\frac{|\alpha|}{\beta} A \qquad 1.1.7.$$

By taking the curl of the above equation it can be shown that it does describe the exclusion of magnetic flux from the specimen; and an effective penetration length,

$$\lambda^2(T) = m^*\beta/4e^2\mu_o|\alpha| \qquad 1.1.8.$$

which describes the spatial variations in the electromagnetic effects, can be defined. Ginzburg and Landau considered the differential equation 1.1.3 in the absence of fields ($A = 0$), and from dimensional arguments, a characteristic length $\xi(T)$ was defined below T_c as

$$\xi(T) = \hbar^2/2m^*|\alpha| \qquad 1.1.9.$$

The coherence length ξ provides the characteristic scale for spatial variations in the order parameter. Consider a normal (n) and superconducting (s) interface, the energy of the interface is dependent on the superconducting volume, $V = A \cdot \xi(T)$ where A is the area of the interface. Since Ψ decreases to zero over a distance of $\xi(T)$, the net Gibbs energy of the interface has a contribution in the form, $(G_n - G_s)A\xi(T)$, and from equation 1.1.9, $|\alpha|$ can be regarded as a regular energy spacing.

The GL coherence length being distinct from Pippard's characteristic length (ξ_0) proposed in 1953. Pippard argued that only electrons within $\simeq k_B T_c$ of E_F (the Fermi Energy) should be important in superconductivity,(local theory), and hence could be estimated from the Uncertainty Principle : $\xi_0 = \alpha\hbar v_F/k_B T_c$ (v_F – Fermi velocity). For T far below the critical transition temperature T_c, $\xi(T) = \xi_0$, but near T_c they are different.

The ratio of the two GL characteristic lengths defines the Ginzburg Landau parameter, $\kappa = \lambda/\xi$. The implications of κ were not fully appreciated until 1957 when Abrikosov[3] used κ to explain Type II superconductivity. He calculated, that in the mixed state (between H_{c1} and H_{c2}) the magnetic flux should penetrate in a regular array of flux tubes, each carrying one quantum of flux. The quantity $\phi_0 = hc/2e = 2.0679 \times 10^{-7}$ gauss $\cdot$ cm^2 is known as the fluxoid, or flux quantum. Flux quantization has been observed[4,5] and the GL theory also predicts, and experiments have confirmed, that each vortex in a type II superconductor contains a single quantum of magnetic flux.

Essentially, most elemental superconductors have GL parameter of $\kappa << 1$, however, by alloying materials and forming compounds, the electron mean free path, ℓ decreases to be much smaller than ξ_0 (a **dirty superconductor**); and hence $\xi \approx \ell$ In the above case where $\xi < \lambda$ we have that the surface energy is negative and the lowest energy state will be attained if the flux is dispersed in very small units throughout the sample. This will allow

for a maximization of the normal – superconductor interface. The crossover from positive to negative surface energy occurs for $\kappa = 1/\sqrt{2}$, as shown by Abrikosov in the original paper[3]. The superconductivity associated with negative surface energy is referred to as **Type II superconductivity**, also called **mixed** or **vortex state**, (sect. 1.1.3.1). The core of the vortex is essentially in the normal state and is usually approximated by a cylinder of radius $\simeq \xi$. On the perimeter of the core, superelectrons screen the magnetic field to a distance $\simeq \lambda$. Since each vortex contains one flux quantum $\psi_o = hc/2e$, the density of flux lines, n, determines the magnetic induction $B = n\psi_o$. This was subsequently confirmed by many experiments[11].

The magnetic phase diagram for Type II Superconductivity is shown below in Figure 1.1.1. Above the $H_{c2}(T)$ curve, the sample is normal. For $H_{c1} < H < H_{c2}$, the superconductor is in the vortex state. Below the $H_{c1}(T)$ curve, all the flux is expelled from the bulk as in a Type I superconductor, leading to what is sometimes referred as the Meissner State. An elementary picture (relation) can be formed between the critical fields, H_{c1} and H_{c2} and the GL length scales in type II superconductors. When the applied field is just above H_{c1}, the field at the vortex core will be $\approx H_{c1}$, radially decreasing to zero over a length $\approx \lambda$. Thus the flux will be $\approx \pi\lambda^2 H_{c1}$ and,

$$H_{c1} \approx \varphi_o/[4]\pi\lambda^2 \qquad 1.1.10.$$

However, if the applied field is just below H_{c2}, the vortices are packed together and each has an effective area $\approx \pi\xi^2$ or,

$$H_{c2} \approx \varphi_o/[2]\pi\xi^2 \qquad 1.1.11.$$

Note: The numerical factors in parenthesis are included for correctness as found from experimental evidence.

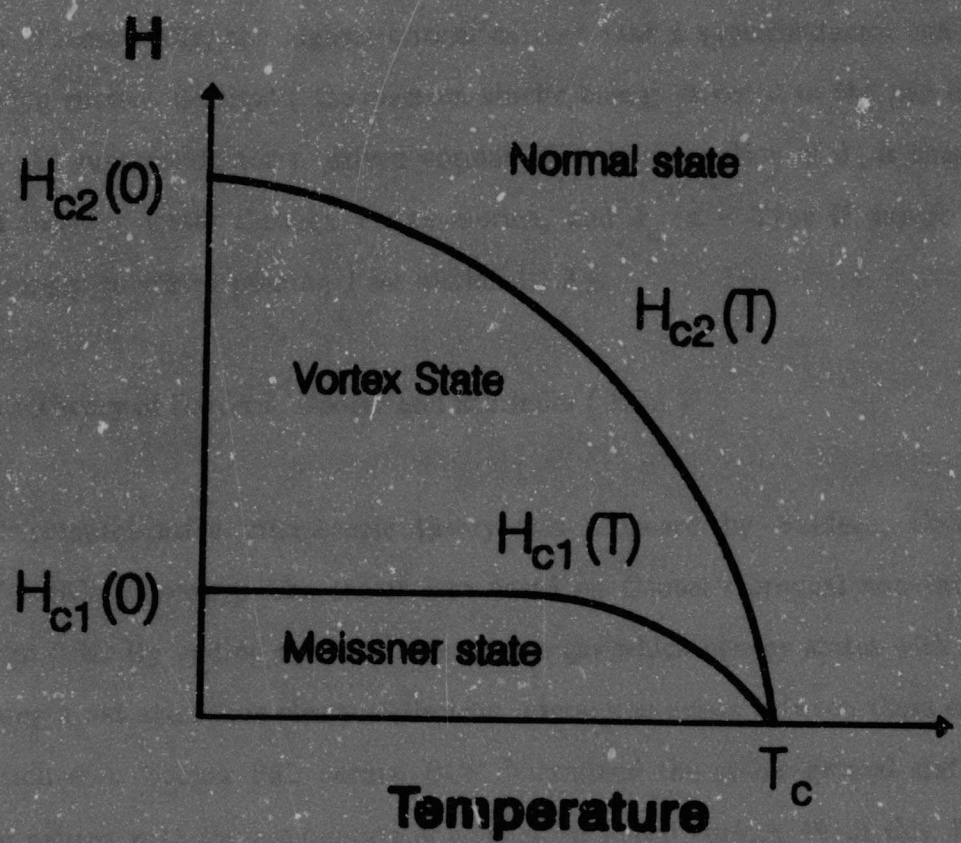


Figure 1.1.1 A schematic representation of the mean field magnetic phase diagram for a Type II superconductor.

The Critical Currents of superconductors became important with the discovery of Type II Superconductivity, when large magnetic fields could be produced with the consumption of almost zero electrical power. The critical current, J_c, is the maximum current density that can be sustained by a superconductor before the particular measurement technique detects dissipation. Theoretically, the highest critical current that a superconductor can carry is the 'depairing current density' (the electron kinetic energy is equal to the gap energy), above this the superconductor is driven normal. The determination of J_c is complicated because of resistive losses through vortex motion, and J_c in a Type II superconductor depends strongly on vortex pinning. (see section 1.1.3).

1.1.2 Theory of Bardeen, Cooper and Schrieffer (BCS)

In 1957 a comprehensive microscopic theory was proposed by Bardeen, Cooper and Schreiffer[6] (BCS Theory). The theory was based on Cooper's original non–interacting Fermi gas at 0 K. By adding two electrons to this gas which occupy states with $k > k_F$, and assuming a net attractive electron–electron interaction exists between these electrons, the formation of a Cooper Pair occurs. BCS determined the stable ground state in the presence of pairing with the assumption of a spherical Fermi surface. With this, BCS was able to predict (sample independent) characteristics of the superconducting state: density of states; energy gap; and isotope effect.

BCS were able to show that there is a second–order phase transition for H = 0, to a new electron state with the transition temperature expressed as

$$k_B T_c = 1.14\hbar\omega_c \exp[-1/N(E_F)V_o] \qquad 1.1.12.$$

where $N(E_F)$ is the density of normal state electrons at the Fermi energy and V_o is the interaction potential between electrons. The cut–off phonon energy $\hbar\omega_c$ is related to the

Debye energy $\hbar\omega_D$, and $\omega_D \propto M^{-1/2}$, where M is the atomic mass. Thus the Isotope effect comes out of the theory namely, $T_c \propto M^{-1/2}$. BCS theory found a gap ($2\Delta(0)$ at 0 K), in the allowed states about E_F. An exaggerated idea of the gap is shown in Figure 1.1.2. The normal–state free electron–like density of states is shown, which at 0K is filled up to $E_F - \Delta(0)$. In the superconductor the energy gap 'forces' allowed states into regions below and above it. The superconducting density of states, $N_S(E)$, for $E > \Delta$ and $E < -\Delta$, is

$$N_S(E) = N(0) \cdot E/(E^2 - \Delta^2)^{1/2} \qquad 1.1.13.$$

For energies within the gap, the density of allowed states is zero.

Importantly, the BCS theory predicted a minimum energy, $E_g(0) = 2\Delta(0)$, necessary to break a Cooper pair (in zero field) and form two quasi–particle excitations:

$$E_g(0) = 2\Delta(0) = 3.528 \cdot k_B T_c \qquad 1.1.14.$$

That is, excited states all have energy at least $|\Delta|$ above the ground state energy E_o. The earliest quasi–particle tunneling experiments[7,8] verified the Energy Gap and values for $2\Delta(0)$ were close to 3.5 for many compound superconductors. The gap vanishes at T_c and for temperatures just below T_c, $\Delta(T)$ can be approximated by:

$$\Delta(T) = A \cdot T_c(1 - T/T_c)^{1/2} \qquad 1.1.15.$$

where A = 3.06. At very low temperatures $\Delta(T)$ is almost independent of temperature The temperature dependence of the gap is illustrated in Figure 1.1.3 below.

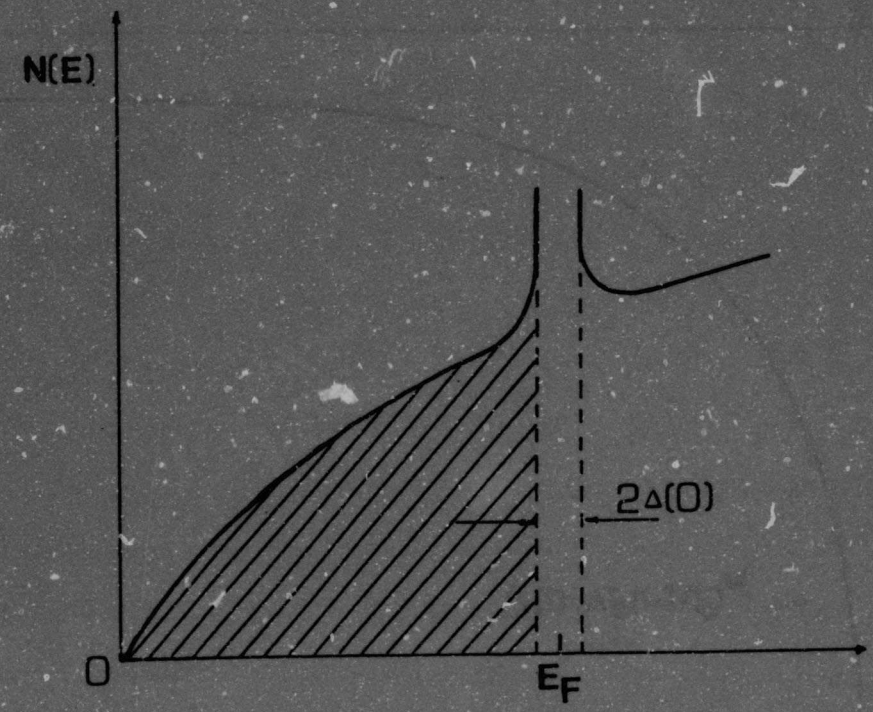


Figure 1.1.2 A normal–state, free electron, quadratic density of states filled with electrons up to E_F–$\Delta(0)$. The superconducting energy gap $2\Delta(0)$ is shown and the allowed states that were in the gap are pushed into regions just above and below the gap. In the diagram the width of the gap is exaggerated around E_F.

Author De Villiers P
Name of thesis Investigation of extended and localised states in a high-temperature superconducting ceramic 1994

PUBLISHER:
University of the Witwatersrand, Johannesburg
©2013

LEGAL NOTICES:

Copyright Notice: All materials on the University of the Witwatersrand, Johannesburg Library website are protected by South African copyright law and may not be distributed, transmitted, displayed, or otherwise published in any format, without the prior written permission of the copyright owner.

Disclaimer and Terms of Use: Provided that you maintain all copyright and other notices contained therein, you may download material (one machine readable copy and one print copy per page) for your personal and/or educational non-commercial use only.

The University of the Witwatersrand, Johannesburg, is not responsible for any errors or omissions and excludes any and all liability for any errors in or omissions from the information on the Library website.